



This work is licensed under a Creative Commons Attribution License (CC BY 4.0).

## Research article

[urn:lsid:zoobank.org:pub:FB07D6FC-0D29-4413-A2D8-BD0039475F61](https://zoobank.org/pub:FB07D6FC-0D29-4413-A2D8-BD0039475F61)

# A revision of the genus *Armillipora* Quate (Diptera: Psychodidae) with the descriptions of two new species

Santiago JAUME-SCHINKEL<sup>1,\*</sup> & Ximo MENGUAL<sup>2</sup>

<sup>1,2</sup>Museum Koenig, Leibniz-Institut zur Analyse des Biodiversitätswandels, Adenauerallee 127, D-53113 Bonn, Germany.

\*Corresponding author: [santijaumes@hotmail.com](mailto:santijaumes@hotmail.com); [s.jaume@leibniz-lib.de](mailto:s.jaume@leibniz-lib.de)

<sup>2</sup> Email: [x.mengual@leibniz-lib.de](mailto:x.mengual@leibniz-lib.de)

<sup>1</sup>[urn:lsid:zoobank.org:author:CB8722CA-9B1E-4BB6-AF0C-1A8BD57CC096](https://zoobank.org/author:CB8722CA-9B1E-4BB6-AF0C-1A8BD57CC096)

<sup>2</sup>[urn:lsid:zoobank.org:author:A509310D-B567-4830-B8A4-BCB139BB8768](https://zoobank.org/author:A509310D-B567-4830-B8A4-BCB139BB8768)

**Abstract.** The genus *Armillipora* Quate is recorded for the first time in Ecuador, with a new geographical record for *Armillipora selvica* Quate, 1996 and the descriptions of two new species, namely *Armillipora muyu* sp. nov. and *Armillipora imitata* sp. nov., doubling the total number of species in the genus. In addition, we make available the first DNA barcodes for the genus, providing a sequence of the 5'-end of the cytochrome *c* oxidase subunit I (COI) gene for *A. imitata*, *A. muyu*, and, *A. selvica*. Moreover, we describe the second known female of the genus and we provide a taxonomical key for the known males of the world. Finally, we build Species Distribution Models and discuss the potential distribution of the genus in the Neotropical region.

**Keywords.** Moth flies, DNA barcode, integrative taxonomy, Neotropical region, new species.

Jaume-Schinkel S. & Mengual X. 2024. A revision of the genus *Armillipora* Quate (Diptera: Psychodidae) with the descriptions of two new species. *European Journal of Taxonomy* 925: 161–178.  
<https://doi.org/10.5852/ejt.2024.925.2459>

## Introduction

The moth fly genus *Armillipora* Quate, 1996 (Diptera: Psychodidae) has only been recorded in the Neotropical region (Quate 1996, 1999; Ježek *et al.* 2020). For many years a single species was known, namely *Armillipora selvica* Quate, 1996. This species was described from Costa Rica (Quate 1996) and recorded in Panama three years later (Quate 1999). More recently, Ježek *et al.* (2020) described a second species from Bolivia, *Armillipora suapiensis* Ježek, Oboňa & Le Pont, 2020, breaking the monotypy of the genus and adding a new geographical record to *A. selvica* from Nicaragua. Up to now, *A. selvica* has been recorded from Central America (Nicaragua, Costa Rica, Panama) and *A. suapiensis* is known only from Bolivia. Besides its scattered known distribution, we do not have information about the larval stages or the adult biology of this genus.

In the present study, we report for the first time the genus *Armillipora* from Ecuador, and we describe two new species based on morphological and molecular characters, bringing the total number of

species of *Armillipora* to four. We also describe the second known female of this genus, which belongs to *Armillipora muyu* sp. nov., and provide a new geographical record for *Armillipora selvica* from Ecuador. Moreover, we make available the first DNA barcodes (the sequences of the 5'-end of the cytochrome c oxidase subunit I or COI gene) for *A. selvica*, *A. imitata* sp. nov., and *A. muyu* and provide an identification key for the world males of *Armillipora*. Finally, we discuss the potential distribution of the genus in the Neotropical region based on our species distribution model.

## Material and methods

### Study area

The Cantón Pedro Vicente Maldonado is located in the Pichincha Province in the northern part of Ecuador, (0°10'00" N, 79°00'00" W) with an average altitude of 600 m a.s.l. The climate is warm-humid with an average annual temperature of 24.5°C and an annual precipitation of 4341 mm. The main vegetation is characterized as pre-mountain rainforest (HPPC 2015).

### Terminology

We follow the general terminology proposed by Cumming & Wood (2017) and Kvifte & Wagner (2017).

### Collection and preparation of specimens

Specimens were collected using a Malaise trap, euthanized and preserved in 96% ethanol, and later stored at -20°C. Specimen preparation was done following the protocol explained by Jaume-Schinkel & Kvifte (2022), with the modification of using the whole specimen for DNA extraction instead of just the thorax.

In the material examined section and at the end of each record the holding institution is stated, and between square brackets ([ ]) the number of the specimen is indicated. The abbreviations used for holding institutions and their equivalents are given below:

- INABIO = Instituto Nacional de Biodiversidad, Quito, Ecuador.
- LACM = Natural History Museum of Los Angeles County, Los Angeles, California, USA.
- ZFMK = Museum Koenig, Leibniz-Institut zur Analyse des Biodiversitätswandels (previously known as Zoologisches Forschungsmuseum Alexander Koenig), Bonn, Germany.

### Genetics

A non-destructive methodology from complete specimens was performed in the facilities of ZFMK with the following workflow: A Qiagen (Hilden, Germany) BioSprint 96 magnetic bead extractor, and the corresponding kits were used following the manufacturers' specifications. We amplified from the 5'-end of the cytochrome c oxidase subunit I (COI) gene using the primers HCO2198-JJ (forward) and LCO1490-JJ (reverse) (Astrin & Stüben 2008). PCR was carried out using a TouchDown PCR (TD-PCR) as proposed by Korbie & Mattick (2008) using a QIAGEN Multiplex PCR Kit. Later the PCR products were shipped to Beijing Genomic Institute (BGI) (China, Hong Kong) for bidirectional sequencing. DNA sequences were assembled, aligned, and cleaned using Geneious Prime ver. 2022.1.1 (Biomatters, Auckland, New Zealand). The total sequence length was set to 658 bp.

We downloaded all the available sequences of the tribe Maruinini from BOLD and we used Geneious Prime ver. 2023 to perform a distance-based neighbor-joining (NJ) analysis using the Jukes-Cantor model. All of the sequences generated for this study can be accessed in BOLD under the Dataset DS-ARMI (available at: <https://doi.org/10.5883/DS-ARMI>). Bootstrap support (BS) values were estimated from 1000 replicates as calculated in Geneious.

### Species Distribution Models

We built a distribution model for the genus using the software MaxEnt ver. 3.4.4 (Phillips *et al.* 2023) with the species' geographical records to infer the potential distribution in the Americas. In MaxEnt ver. 3.4.4 we used all the records of the genus as a single biological entity to evaluate the distribution model for the genus, instead of using each species separately. The resulting map was trimmed to North America, Central America, and South America. Climate variables were obtained from WorldClim (Fick & Hijmans 2017). Geographic coordinates used for the analysis were extracted from the localities reported in the literature and museum collection databases. Localities are summarized in Table 1. For the records without exact coordinates in the literature, we used Google® Earth to search for the reported locality and obtain proxy coordinates and compared them with the coordinates in the collection data base. After comparison, if coordinates did not match, we adjusted them to have at most a difference of  $\pm 50$  meters between both.

### Results

Class Insecta Linnaeus, 1758  
 Order Diptera Linnaeus, 1758  
 Suborder Psychodomorpha Hennig, 1968  
 Family Psychodidae Newman, 1834  
 Subfamily Psychodinae Newman, 1834  
  
 Genus *Armillipora* Quate, 1996

*Armillipora* Quate, 1996: 29. Type species *Armillipora selvica* Quate, 1996 (by original designation).

*Armillipora* – Ježek *et al.* 2020: 418 (updated diagnosis, redescription of type species, and description of new species).

### Differential diagnosis

The genus *Armillipora* has been placed in the tribe Maruinini Enderlein, 1937 based on the presence in the wing of a radial fork being basal to the medial fork and both forks located basally on the wing, as well as the broad and dorsally flattened shape of the ejaculatory apodeme (Quate 1996; Kvitte 2018; Ježek *et al.* 2020). At first glance, species of *Armillipora* resemble those of *Alepia* Enderlein, 1937 and *Platyplastinx* Enderlein, 1937 mainly by the wing maculation and the presence of two different types of tenacula on the epandrial appendage (see Quate 1996: fig. 11; Ježek *et al.* 2020: figs 1–20; Jaume-Schinkel *et al.* 2022: figs 1–15; Jaume-Schinkel & Kvitte 2022: figs 1–16). But species of *Armillipora* can be easily differentiated using characteristics of the male genitalia as follows: the characteristic shape of the irregularly-asymmetrical epandrial appendage (not irregularly asymmetrical in *Alepia* and *Platyplastinx*), the long accessory tenacula (long in *Alepia*, but short in *Platyplastinx*) with a group of short cylindrical tip-folded tenacula (not present in *Alepia* and *Platyplastinx*), with the absence of apical tenacula (usually none, one or more apical tenacula in *Alepia* and *Platyplastinx*), the lack of gonostyli and the gonocoxites fused in *Armillipora* (gonostyli present and gonocoxites usually not fused in *Alepia* and *Platyplastinx*), and the absence of the aedeagal sheath (present in *Alepia*, but absent in *Platyplastinx*) (see Ježek *et al.* 2020). Females of *Armillipora* can be differentiated of those of *Alepia* and *Platyplastinx* by the following characters: antennal flagellomeres with double circle of teardrop-shaped pores in the center, although less conspicuous than males they are present in *Armillipora* (absent in *Alepia* and *Platyplastinx*); *Armillipora* with the subgenital plate longer than wide (subgenital plate length variable in *Alepia*, usually about the same length as its width in *Platyplastinx*), with apical lobes separated by a broad concavity (concavity is broader than twice the length of the apical lobe) with a pair of long spines

on apical margin of concavity (apical lobes not separated by broad concavity (concavity being less than the length of apical lobe) and pair of long spines on apical margin of concavity absent in *Alepia* and *Platyplastinx*).

### Biology

To date, nothing is known about the immature stages and the biology of the species of *Armillipora*. Given the known information about the tribe Maruinini, it is expected that larvae of *Armillipora* breed in some aquatic or semi-aquatic environment.

### Species included

*Armillipora imitata* sp. nov., *A. muyu* sp. nov., *A. selvica* Quate, 1996, *A. suapiensis* Ježek, Oboňa & Le Pont 2020. Species distribution is shown in Table 1.

#### *Armillipora imitata* sp. nov.

[urn:lsid:zoobank.org:act:41F1459A-4F5D-41EF-B205-BE0EB30AC37E](https://zoobank.org/act:41F1459A-4F5D-41EF-B205-BE0EB30AC37E)

Figs 1–2

### Differential diagnosis

*Armillipora imitata* sp. nov. is very similar to *A. muyu* sp. nov. and *A. selvica* but the three can be differentiated as follows: in *A. selvica* the interocular suture has a short posterior spur (posterior spur absent in *A. imitata* and in *A. muyu*); one conical apical and one spiniform tooth at the apex of labella in *A. imitata* (only one conical apical teeth in *A. selvica*; one preapical spiniform and one apical claw-shaped in *A. muyu*); *A. imitata* has six apical setae at the apex of gonocoxites (three to four setae placed on a preapical lump in *A. muyu*, and three to four preapical setae in *A. selvica*); the gonocoxal condyles is not triangular and not protruding beyond the base of the ejaculatory apodeme in *A. imitata* and *A. muyu* (the sclerite is triangular and protruding beyond the base of ejaculatory apodeme in *A. selvica*).

### Etymology

The species epithet ‘*imitata*’ derives from the Latin word ‘*imitātus*’ (feminine ‘*imitāta*’) referring to its similarity with other species. It is to be treated as an adjective.

### Material examined

#### Holotype

ECUADOR – **Pichincha** • ♂; Parroquia Pedro Vicente Maldonado, Roadway to Pachijal; 0.11561° N, 78.95805° W; alt. 750 m; 1–9 Feb. 2022; Kilian and Isabel leg.; INABIO [ZFMK-DIP-00097935, ZFMK-TIS-2637091].

#### Paratypes

ECUADOR • 1 ♂; same collection data as for holotype; ZFMK [ZFMK-DIP-00097934, ZFMK-TIS-2637173] • 1 ♂; same collection data as for holotype; ZFMK [ZFMK-DIP-00097931, ZFMK-TIS-2637132].

### Description

MEASUREMENTS in mm (n = 3). Wing length: 2.19 (2.20–2.18), width: 1.00 (1.05–0.98). Head length: 0.50 (0.52–0.48), width: 0.55 (0.56–0.52). Antennal segments: scape: 0.10 (0.10–0.10); pedicel: 0.06 (0.06–0.06); flagellomeres 1–5: 0.15 (0.15–0.11), flagellomeres 6–10: 0.12 (0.15–0.13). Palpal segment 1: 0.07 (0.07–0.07); palpal segment 2: 0.08 (0.09–0.08); palpal segment 3: 0.08 (0.08–0.08); palpal segment 4: 0.14 (0.15–0.14).

**Male**

**HEAD.** About 1.10 times as wide as long; eye bridge separated by 1 facet's diameter, with four rows of facets, interocular suture as sclerotized, almost straight line; frontal patch of alveoli divided. Antennal scape about 1.5 times as long as pedicel, almost cylindrical; pedicel spherical, smaller than scape; flagellomeres fusiform and longer than scape, with scattered setae on surface, setae almost as long as flagellomere bearing them, each flagellomere with two rings of teardrop-shaped pores, apical flagellomeres absent in examined material, maximum number of flagellomeres present: five; ascoids indistinguishable in examined material. Palpal segments cylindrical, palpal proportions: 1.0:1.1:1.1:1.8, last palpal segment corrugated; labium without any strong sclerite; labella elongated and irregularly shaped scattered setae on surface, with one apical spiniform tooth on each.

**THORAX.** Without allurement organs. With single patch of alveoli in paratergite and anteprepronotum; all coxae with stripe of one to two rows of alveoli. Wing length about two times its width; wing membrane brown-infuscated, with lightened spots in between apex of longitudinal veins, and with light triangular-shaped spot between origin of  $R_1$  and  $R_{2+3}$  (Fig. 1B); subcostal vein short ending beyond origin of  $R_5$ ; junction of  $R_{2+3}$  basal to junction of  $M_{1+2}$ , not joining  $R_4$ ; origin of  $M_{1+2}$  basal to origin of  $R_{2+3}$ ;  $R_5$  ending at wing apex;  $CuA_2$  faintly ending at wing margin.

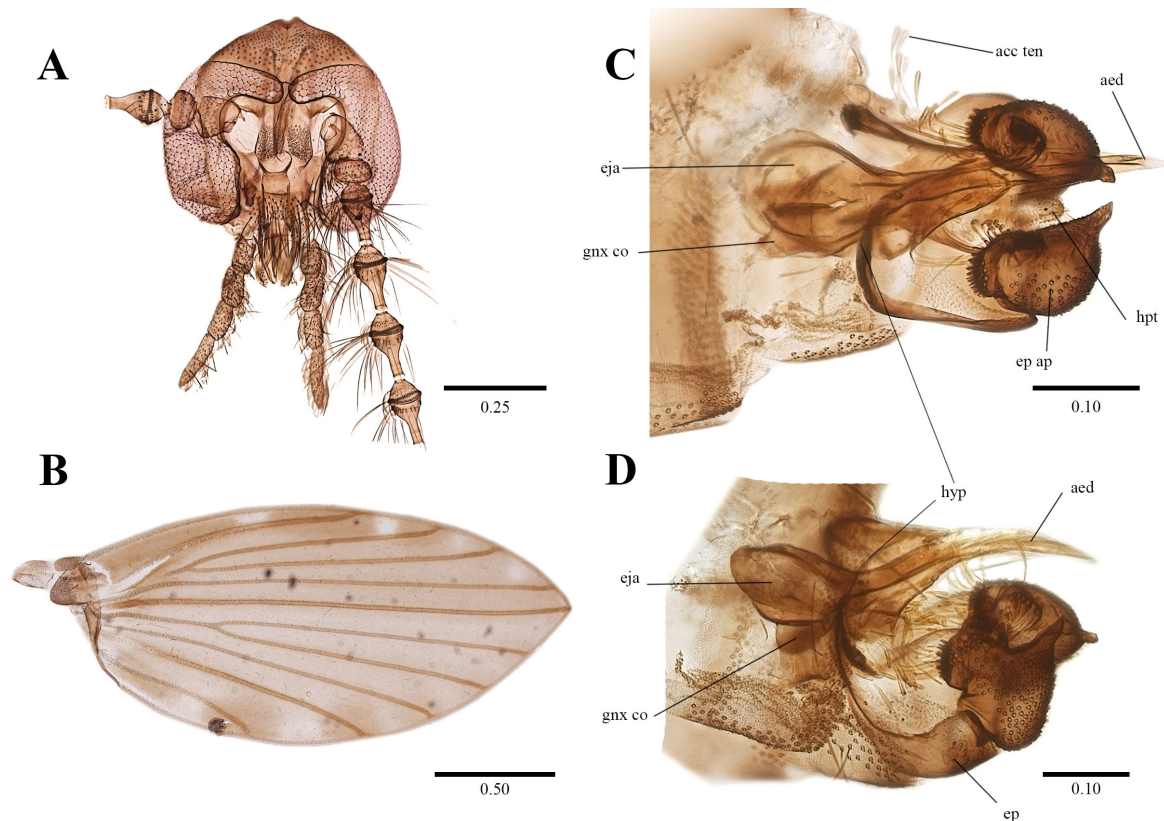


**Fig. 1.** *Armillipora imitata* sp. nov. **A–C.** Holotype, ♂ (ZFMK-DIP-00097935). **D.** Paratype, ♂ (ZFMK-DIP-00097934). **A.** Head. **B.** Wing. **C.** Genitalia in dorsal view. **D.** Genitalia in ventral view. Scale bars in mm. Abbreviations: acc ten = accessory tenacula; aed = aedeagus; eja = ejaculatory apodeme; ep = epandrium; ep ap = ependrial appendages; gnx co = gonocoxal condyles; hpt = hypoproct; hyp = hypandrium.

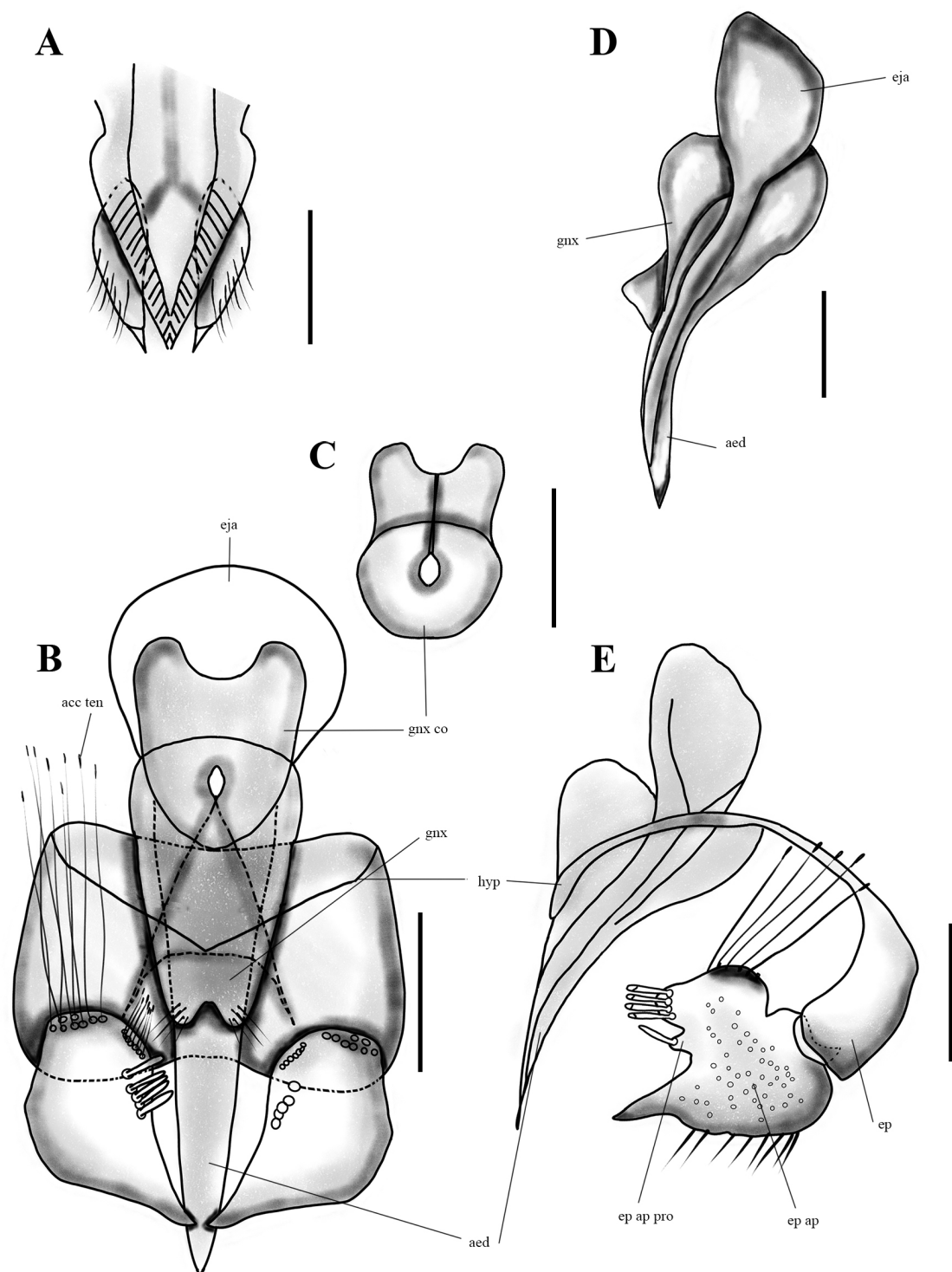


**Fig. 2.** *Armillipora imitata* sp. nov. **A–C.** Holotype, ♂ (ZFMK-DIP-00097935). **D–E.** Paratype, ♂ (ZFMK-DIP-00097934). **A.** Mouthparts. **B.** Genitalia in ventral view. **C.** Gonocoxal condyles. **D.** Aedeagus in lateral view. **E.** Genitalia in lateral view. Scale bars = 0.10 mm. Abbreviations: acc ten = accessory tenacula; aed = aedeagus; eja = ejaculatory apodeme; ep = epandrium; ep ap = epandrial appendage; ep ap pro = epandrial appendage projection; gnx co = gonocoxal condyles; hyp = hypandrium.

**TERMINALIA** (Figs 1C–D, 2B–E). Hypandrium in dorsal view V-shaped, sclerotized and joining base of gonocoxites, in lateral view hypandrium looks membranous (Figs 1C, 2B, E) with sclerotized margin; gonocoxites joining at apex forming U-shaped sclerite, with concavity at lower margin. Gonocoxite sclerite placed above aedeagal complex. On each side of sclerite is a preapical cluster of six setae (Figs 1C, 2B); gonostyli absent; aedeagus in dorsal view straight, as single sclerite, no discernible parameres. In lateral view, aedeagus apex curved towards epandrial appendage (Figs 1D, 2E); ejaculatory apodeme about half length of aedeagus, in dorsal view basal margin rounded and slightly concave in middle, in lateral view, ejaculatory apodeme looks like half-circle, with basal margin convex; gonocoxal condyles fitting in concavity on underside of ejaculatory apodeme, not triangular-shaped and not protruding beyond base of ejaculatory apodeme; epandrium rectangular, wider than long, with more sclerotization at margins, anterior and posterior margins with medial concavity; hypoproct tongue-shaped (Fig. 1C), shorter than epandrium and covered with small setulae, epiproct not visible in examined material; epandrial appendage barely hemispherical, prolonged and tapering distally, covered with small setae; epandrial appendage lacking apical tenacula. In dorsal view (Figs 1C, 2B), line of five short and cylindrical tenacula, with folded tips; in lateral view, (Figs 1D, 2E) first four tenacula close to each other, last tenaculum separated and located in projection of epandrial appendage, this projection not visible in dorsal view; epandrial appendage possesses additional patch of long accessory tenacula basally concentrated in darkened patch, these accessory tenacula being as long as or longer than epandrium (Figs 1C, 2B).

#### **Female**

Unknown.

#### **Distribution**

Only known from the type locality in Ecuador.

#### **Genetics**

Three specimens were successfully sequenced (ZFMK-TIS-2637091, ZFMK-TIS-2637173, and ZFMK-TIS-00097931). The maximum intraspecific uncorrected pairwise distance for COI sequences was 1.06 % or 7 bp. GenBank accession numbers are: OQ706375; OQ706387; OQ706388.

#### *Armillipora muyu* sp. nov.

[urn:lsid:zoobank.org:act:F00EDE09-9B2D-4114-971F-6168D54DC6AF](https://zoobank.org/urn:lsid:zoobank.org:act:F00EDE09-9B2D-4114-971F-6168D54DC6AF)

Figs 3–5

#### **Differential diagnosis**

Male: see differential diagnosis under *A. imitata* sp. nov.

#### **Etymology**

The species epithet ‘muyu’ derives from the Quechuan word ‘*muyu*’, meaning circle and referring to the circular shape of the base of the ejaculatory apodeme. It is to be treated as a name in apposition.

#### **Material examined**

##### **Holotype**

ECUADOR – **Pichincha** • ♂; Parroquia Pedro Vicente Maldonado, Roadway to Pachijal; 0.11882° N, 78.95802° W; alt. 750 m; 1–9 Feb. 2022; Kilian, Isabel leg.; INABIO [ZFMK-DIP-00081675, ZFMK-TIS-2636967].

### Paratypes

ECUADOR • 1 ♂; same collection data as for holotype; ZFMK [ZFMK-DIP-00081976, ZFMK-TIS-636968] • 1 ♂; same collection data as for holotype; ZFMK [ZFMK-DIP-00081977 ZFMK-TIS-2636969] • 1 ♂; same collection data as for holotype; ZFMK [ZFMK-DIP-00097932, ZFMK-TIS-2637146] • 1 ♀; same collection data as for holotype; ZFMK [ZFMK-DIP-00081836, ZFMK-TIS-2636973] • 1 ♂; same collection data as for holotype; 25–28 Jan. 2020; 0.11561° N, 78.95805° W; ZFMK [ZFMK-DIP-00081975, ZFMK-TIS-2636967] • 1 ♂; same data as for preceding; INABIO [ZFMK-DIP-00081667, ZFMK-TIS-2629905].

### Description

#### Male

MEASUREMENTS in mm (n = 5). Wing length 1.85 (2.00–1.65), width 0.84 (0.90–0.71); head length 0.40 (0.45–0.37), width 0.47 (0.52–0.41). Antennal segments: scape: 0.09 (0.10–0.08); pedicel: 0.05 (0.06–0.05); flagellomeres 1: 0.12 (0.12–0.11), flagellomeres 2–5: 0.12 (0.13–0.11). Palpal segment 1: 0.05 (0.06–0.05); palpal segment 2: 0.06 (0.08–0.07); palpal segment 3: 0.04 (0.07–0.06); palpal segment 4: 0.12 (0.13–0.12).

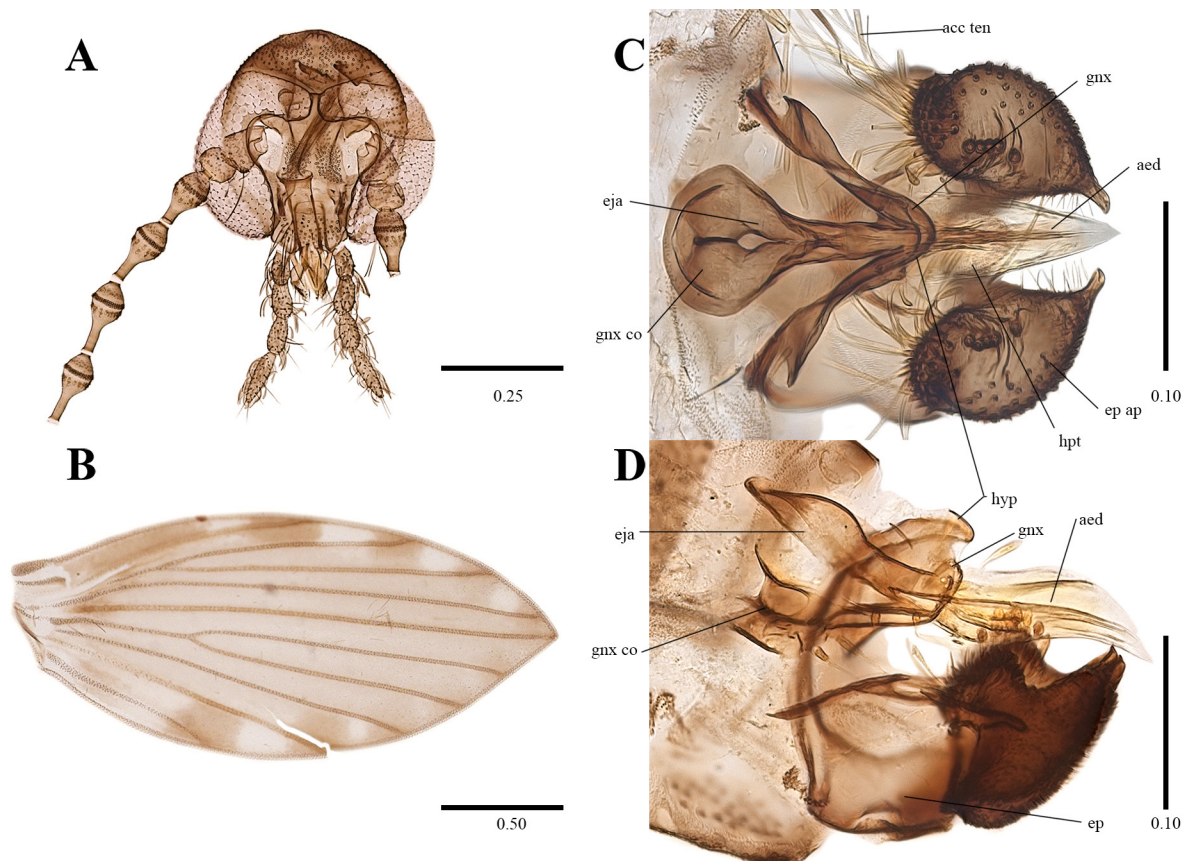


**Fig. 3.** *Armillipora muyu* sp. nov. **B, C.** Holotype, ♂ (ZFMK-DIP-00081675). **A, D.** Paratype, ♂ (ZFMK-DIP-00081976). **A.** Head. **B.** Wing. **C.** Genitalia in ventral view. **D.** Genitalia in lateral view. Scale bars in mm. Abbreviations: acc ten = accessory tenacula; aed = aedeagus; eja = ejaculatory apodeme; ep = epandrium; ep ap = epandrial appendage; gnx = gonocoxite; gnx co = gonocoxal condyles; hpt = hypoproct; hyp = hypandrium.

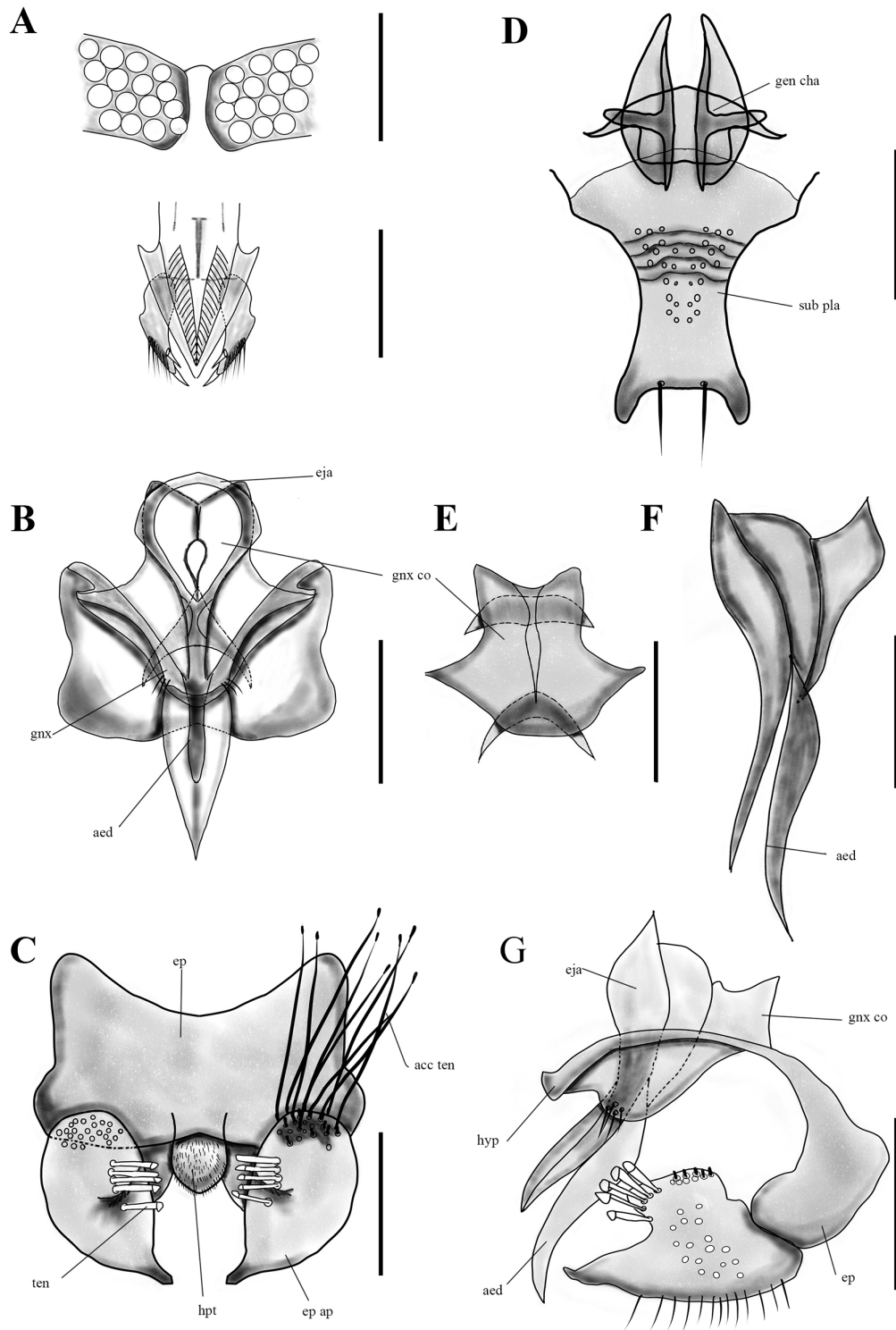


**Fig. 4.** A–C, E–G: ♂. D: ♀. *Armillipora muyu* sp. nov. **A.** Eye bridge and mouthparts. **B.** Aedeagal complex. **C.** Epandrium and epandrial appendages. **D.** Female genitalia. **E.** Gonocoxal condyles. **F.** Aedeagus in lateral view. **G.** Genitalia in lateral view. Scale bars = 0.10 mm. Abbreviations: acc ten = accessory tenacula; add scl = additional sclerite of ejaculatory apodeme; aed = aedeagus; eja = ejaculatory apodeme; ep = epandrium; gen cha = genital chamber; gnX = gonocoxite; gnX co = gonocoxal condyles; hpt = hypoproct; hyp = hypandrium; sub pla = subgenital plate; ten = tenacula.

HEAD. About 1.15 times as wide as long; eye bridge separated by one or less than one facet diameters, with four rows of facets, five on broadest part of eye bridge in some specimens; interocular suture as sclerotized, slightly curved line, without posterior spur; frontal patch of alveoli divided. Antennal scape about 1.8 times as long as pedicel, almost cylindrical; pedicel

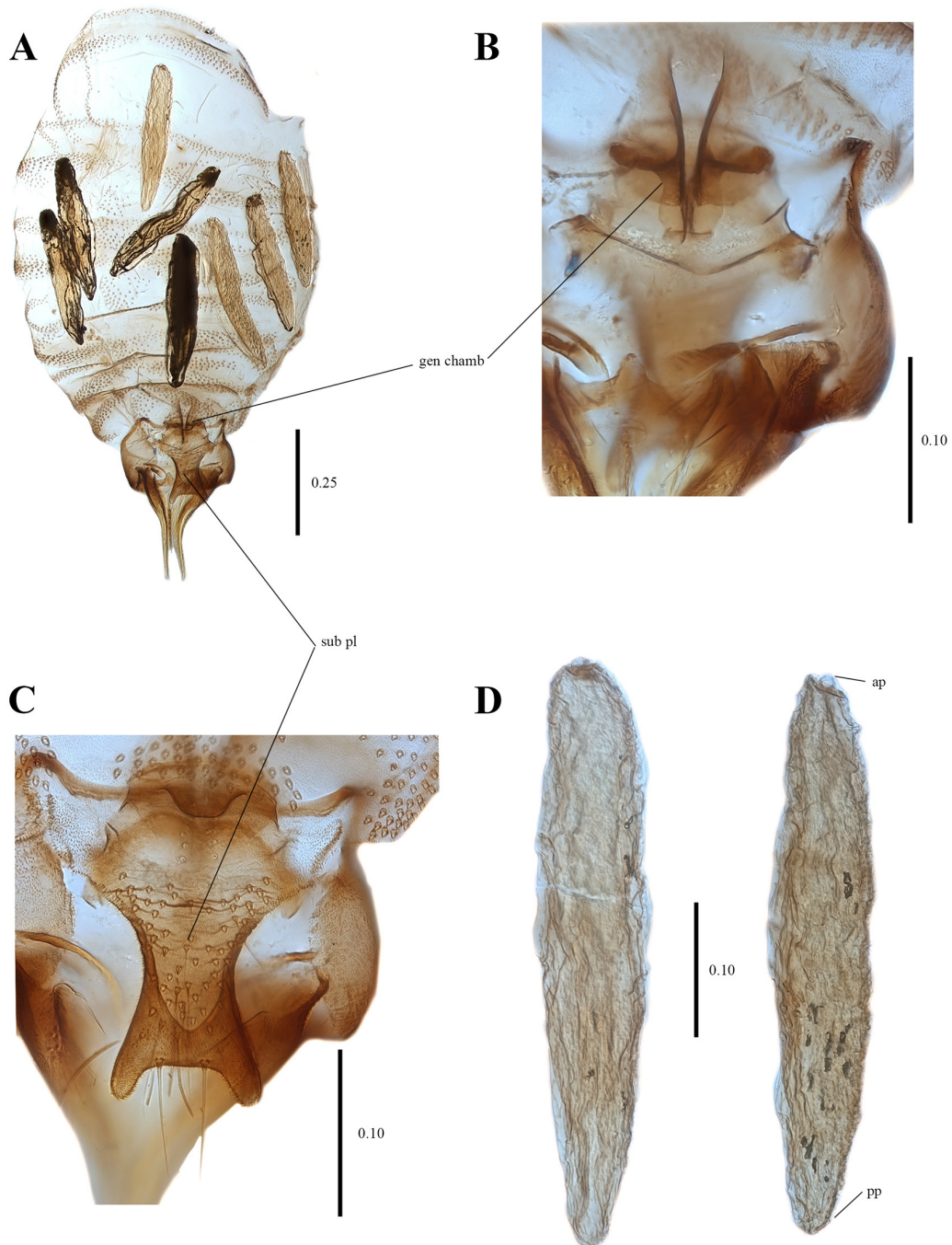


**Fig. 5.** *Armillipora muyu* sp. nov., paratype, ♀ (ZFMK-TIS-2636973). **A.** Abdomen. **B.** Genital chamber. **C.** Subgenital plate. **D.** Eggs. Scale bars in mm. Abbreviations: ap = anterior pole; gen chamb = genital chamber; pp = posterior pole; sub pl = subgenital plate.

spherical, smaller than scape; flagellomeres fusiform and longer than scape, with scattered setae on surface, setae almost as long as flagellomere bearing them, each flagellomere with two rings of teardrop-shaped pores, apical flagellomeres absent in examined material, maximum number of flagellomeres present: 5; ascoids indistinguishable in reviewed material. Palpal segments cylindrical, palpal proportions: 1.0:1.2:1.1:2.0, last palpal segment not corrugated; labium without any strong sclerite; labella elongated and irregularly shaped with six to eight setae concentrated in darkened spot at lower outer margin, with one pre-apical spiniform and one apical spiniform tooth on each.

THORAX. Allurement organs absent, with single patch of alveoli in paratergite and anteprepronotum; all coxae with stripe of one to two rows of alveoli. Wing length about two times its width; wing membrane brown-infuscated, with darkened spots on apex of longitudinal veins (Fig. 1B); subcostal vein short ending beyond origin of  $R_5$ ; junction of  $R_{2+3}$  basal to junction of  $M_{1+2}$ , not joining  $R_4$ , origin of  $M_{1+2}$  basal to origin of  $R_{2+3}$ ;  $R_5$  ending at wing apex;  $CuA_2$  faintly ending at wing margin.

TERMINALIA (Figs 3C–D, 4B–C, E–G). Hypandrium in dorsal view U-shaped, and sclerotized, joining base of gonocoxites. In lateral view hypandrium looks membranous (Fig. 3D) with sclerotized margin; gonocoxites joining at apex forming V-shaped sclerite placed above aedeagal complex, each with preapical lateral lump with cluster of three to four setae (Figs 3C, 4B), gonostyli absent; aedeagus in dorsal view straight, as single sclerite, no discernible parameres. In lateral view, aedeagus has curved apex towards hypandrium (Fig. 4G); ejaculatory apodeme about same length as aedeagus, in dorsal view, basal margin rounded and slightly concave in middle, in lateral view, ejaculatory apodeme looks like half-circle, with basal margin concave; gonocoxal condyles fitting in concavity on underside of ejaculatory apodeme, not triangular-shaped and not protruding beyond base of ejaculatory apodeme; epandrium rectangular, slightly wider than long, with more sclerotization at margins, lateral margins with slight concavity in middle; hypoproct tongue-shaped, shorter than epandrium and covered with small setulae, epiproct shorter than hypoproct; epandrial appendage barely hemispherical, prolonged and tapering distally, covered with small setae, lacking apical tenacula but with line of five short and cylindrical tenacula, with folded tips, and additional patch of long accessory tenacula basally concentrated in darkened patch, these accessory tenacula being as long as or longer than epandrium (Figs 3C, 4C).

#### Female (Figs 4D, 5A–C)

Similar to male except for following characteristics: two rings of teardrop-shaped pores in flagellomeres not as well defined as in males being more scattered and smaller, flagellomeres smaller than male flagellomeres. Wing length equals 2.55 times its width. Subgenital plate long, lateral margins concave in middle, and apical margin has rectangular concavity, with two setae at margin of concavity in addition to scattered setae on surface (Figs 4D, 5A, C); cerci about 1.5 times as long as subgenital plate (Fig. 5A), each with scattered setae on basal surface; genital chamber appears asymmetrical; however, this might be due to bad slide preparation, nonetheless, structures can be seen in Figs 4D, 5B. Female of *Armillipora muyu* sp. nov. can be easily differentiated from female of *Armillipora selvica* by following characters: apical concavity in subgenital plate rectangular (rounded in *A. selvica*); genital chamber with two anterior lobes in *Armillipora muyu* as in Figs 4D, 5B (genital chamber quadrate without anterior lobes in *A. selvica*, see Quate 1996: fig. 11d).

#### Egg (Fig. 5D)

Female specimen contained eggs inside abdomen, shape of eggs long-ovoid, being five times as long as wide; general appearance of membrane corrugated, with irregular folds across entire surface; anterior pole of eggs has semi-circular small projection.

### Remarks

In the paratype ZFMK-DIP-00081667, the palpal segments are missing; the thorax and right wing were used for DNA extraction and are not present in the slide.

### Distribution

Only known from the type locality in Ecuador.

### Genetics

Six specimens were successfully sequenced (ZFMK-TIS-2636967, ZFMK-TIS-636968, ZFMK-TIS-2636969, ZFMK-TIS-2636973, ZFMK-TIS-2637146, ZFMK-TIS-2629905). The maximum intraspecific uncorrected pairwise distance for COI sequences was 3.04 % or 20 bp. Genbank accession numbers are: OQ706383, OQ706381, OQ706385, OQ706386, OQ706378, OQ706376.

### *Armillipora selvica* Quate, 1996

Fig. 6

*Armillipora selvica* Quate, 1996: 29 (description). – Quate 1999: 427 (a new geographical record). – Ježek *et al.* 2020: 419 (redescription and a new geographical record).

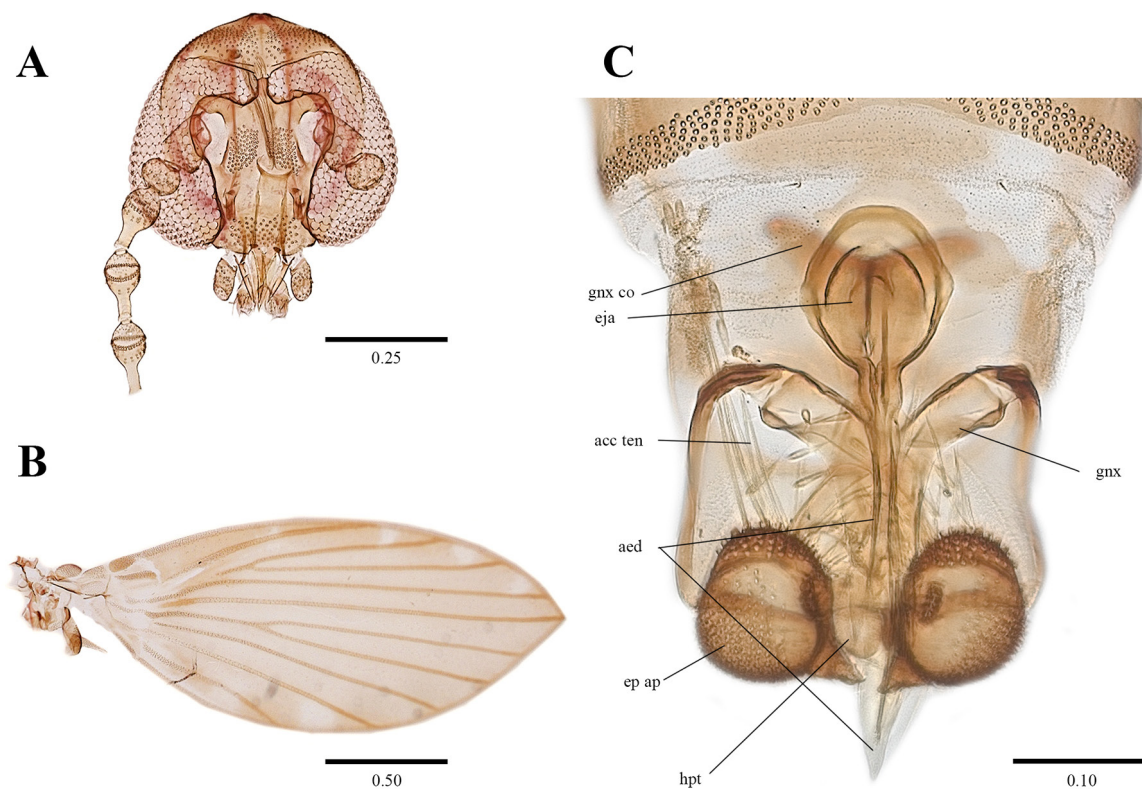


**Fig. 6.** *Armillipora selvica* Quate, 1996, ♂ (ZFMK-TIS-2629865). **A.** Head. **B.** Wing. **C.** Genitalia in ventral view. Scale bars in mm. Abbreviations: acc ten = accessory tenacula; aed = aedeagus; eja = ejaculatory apodeme; ep ap = epandrial appendage; gnx = gonocoxite; gnx co = gonocoxal condyles; hpt = hypoproct.

### Differential diagnosis

See differential diagnosis under *A. imitata* sp. nov.

### Material examined

ECUADOR – **Pichincha** • 1 ♂; Pedro Vicente Maldonado, Parroquia Pedro Vicente Maldonado, Roadway to Pachijal; 0.11882° N, 78.95802° W; alt. 750 m; 1–9 Feb. 2022; Kilian and Isabel leg.; ZFMK [ZFMK-DIP-00097930, ZFMK-TIS-2637093] • 1 ♂; same collection data as for preceding; INABIO [ZFMK-DIP-00097933, ZFMK-TIS-2637154] • 1 ♂; same collection data as for preceding; ZFMK [ZFMK-DIP-00081837, ZFMK-TIS-2636974] • 1 ♂; same data as for preceding; 30 Dec. 2021–5 Jan. 2022; ZFMK [ZFMK-DIP-00081968, ZFMK-TIS-2636960] • 1 ♂; same collection data as for preceding; 25–28 Jan. 2020; ZFMK [ZFMK-DIP-00081670, ZFMK-TIS-2629865].

### Distribution

Nicaragua (Ježek *et al.* 2020), Costa Rica (Quate 1996), Panama (Quate 1999), and Ecuador (this publication, new record).

### Genetics

Five specimens were successfully sequenced (ZFMK-TIS-2637093, ZFMK-TIS-2637154, ZFMK-TIS-2636960, ZFMK-TIS-2629865, and ZFMK-TIS-2636974). The maximum intraspecific uncorrected pairwise distance for COI sequences was 4.10 % or 27 bp. Genbank accession numbers are: OQ706382; OQ706380; OQ706377; OQ706379; OQ706384.

### *Armillipora suapiensis* Ježek, Oboňa & Le Pont, 2020

*Armillipora suapiensis* Ježek, Oboňa & Le Pont, 2020: 422 (description).

### Differential diagnosis

Based on the original description of Ježek *et al.* (2020), *Armillipora suapiensis* can be easily separated from all the other species of the genus by the following characteristics: eye bridge with five rows of facets (four rows of facets in other species); more than six cylindrical tenacula present in epandrial appendage in *A. suapiensis* (six or less cylindrical tenacula present in other species); gonocoxites not fused in *A. suapiensis* (fused in other species); parameres not fused and outwardly curved in *A. suapiensis* (fused in other species), aedeagus around twice as long as ejaculatory apodeme in *A. suapiensis* (about same length of ejaculatory apodeme in other species); ejaculatory apodeme with pointed anterior margin in *A. suapiensis* (rounded anterior margin in other species) (see Ježek *et al.* 2020).

### Material examined

None.

### Distribution

Bolivia (Ježek *et al.* 2020).

### Key to the males of *Armillipora*

1. Eye bridge with five facet rows; more than six tenacula on the epandrial appendage; gonocoxites not fused..... *A. suapiensis* Ježek, Oboňa & Le Pont, 2020
- Eye bridge with four facet rows; six or fewer tenacula on the epandrial appendage; gonocoxites fused..... 2

2. The interocular suture with short posterior spur (Fig. 6A); gonocoxal condyles triangular-shaped and protruding beyond base of ejaculatory apodeme ..... *A. selvica* Quate, 1996
  - Interocular suture without posterior spur (Figs 1A, 3A); gonocoxal condyles not triangular-shaped and not protruding beyond base of ejaculatory apodeme ..... 3
3. Gonocoxites fused, forming U-shaped sclerite, with concavity at lower margin, gonocoxites without preapical lumps, each containing six preapical setae (Figs 1C, 2B); epandrial appendage in lateral view with line of four short and cylindrical tenacula, with additional tenaculum placed on separate projection of epandrial appendage (Fig. 2E) ..... *A. imitata* sp. nov.
  - Gonocoxites fused, forming V-shaped sclerite (Figs 3C, 4B), each with preapical lump, each containing three to four setae; epandrial appendage in lateral view with line of five short and cylindrical tenacula without additional projections on epandrial appendage (Fig. 4G) .....  
..... *A. muyu* sp. nov.

### Genetics

Barcoded specimens of *Armillipora imitata* sp. nov. have an intraspecific uncorrected pairwise distance for COI sequences of 1.06 %. Similarly, specimens of *A. muyu* sp. nov. have an uncorrected pairwise distance of 3.04 %, and specimens of *A. selvica* show an uncorrected pairwise distance 3.80 %. The interspecific uncorrected pairwise distances are higher, for instance *A. muyu* has a maximum interspecific uncorrected pairwise distance of 9.57 % (9.57–9.11 %) with *A. imitata* and 10.03 % (10.03–8.81 %) with *A. selvica*. In a similar manner, *A. imitata* has a maximum uncorrected pairwise distance of 5.92 % (5.92–5.02) compared to *A. selvica* (Table 2). All sequenced specimens cluster well into morphological taxa in the NJ tree (Fig. 7).

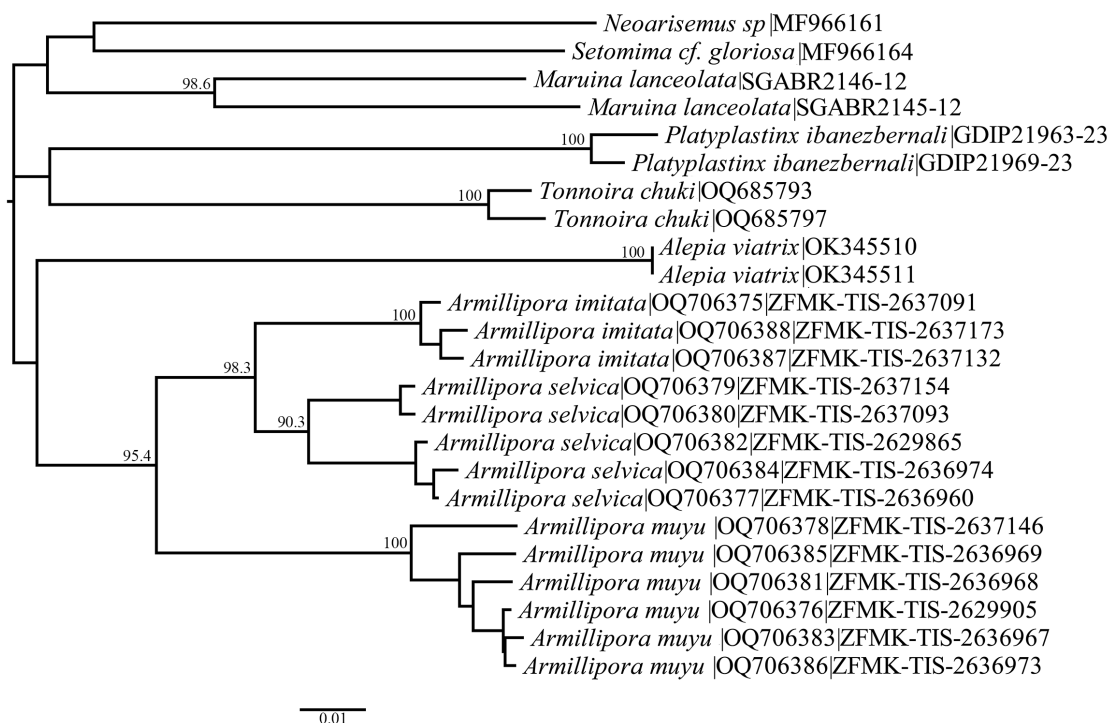


**Fig. 7.** Neighbor-joining tree using Jukes-Cantor model based on the COI sequences of the examined material and sequences downloaded from BOLD. The name for each specimen has the name of the species | BOLD/GenBank accession number | sample ID. Bootstrap support values are given at the nodes.

### Species distribution model

We gathered a total of 76 geographical records for all the species of *Armillipora* (*A. imitata* sp. nov. n = 3; *A. muyu* sp. nov. n = 7; *A. selvica* n = 55; and *A. suapiensis* n = 11), mainly from the original descriptions. Thirty-six records had exact geographical coordinates, while 40 records were lacking the exact geographical coordinates and these were adjusted based on the reported locality (Table 1).

The species of *Armillipora* are currently reported in five countries, namely Bolivia, Costa Rica, Ecuador, Nicaragua, and Panama (Table 1), and our model shows that the genus can be present in several more countries in the Neotropical region, extending towards North America (Fig. 8). Still, the highest probability of presence is concentrated in Central America and northern South America (Fig. 8).

### Discussion

Species of *Armillipora* are morphologically very similar-looking to each other and the differences are subtle even with slide-mounted specimens. Our results with DNA barcodes prompt us to think that morphological determination can be complemented using COI barcodes with good species delimitation

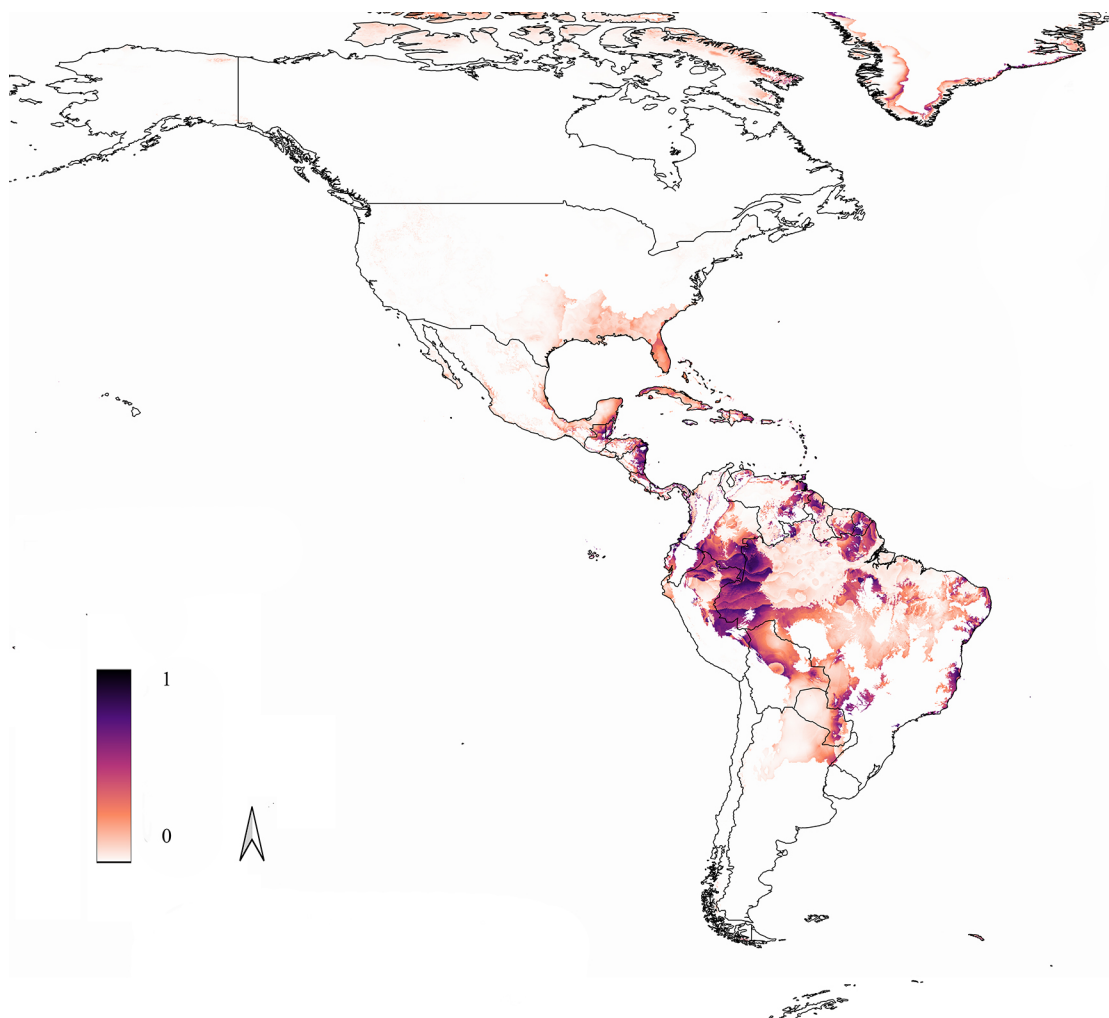


**Fig. 8.** Heat map resulting from the Species Distribution Model using MaxEnt, where 1 is equal to the highest probability of distribution, while 0 is the lowest probability.

results. In other words, we think that morphological determination in combination with DNA barcodes is a good way to determine species of the genus *Armillipora*. In the Neotropical region, however, there is a gap in the number of known species (Linnean shortfall) in combination with a poorly documented geographic distribution (Wallacean shortfall). Both shortfalls with the combination of an absent DNA barcode reference library and only a handful of DNA barcodes generated from the Neotropical region lead to a lack of important information for an integrative taxonomy approach, and future species delimitation techniques could provide valuable information for the genus and for the subfamily Psychodinae in the Neotropics, in general.

Species distribution models do well in predicting the occurrence of many species (Lee-Yaw *et al.* 2021), even dealing at genus level (Stas *et al.* 2020), and our inferred distribution model (Fig. 7) shows that *Armillipora* could be found in several other countries than the ones from which the genus is currently reported (e.g., Brazil, Colombia, French Guyana, Guyana, Peru, Surinam, Venezuela). Following the proposed biogeographic regionalization of Morrone (2014: fig. 12) it can be expected to find the genus in the Mexican Transition Zone, the Antillean subregion, Brazilian subregion, Mesoamerican dominion, Pacific dominion, Boreal Brazilian dominion, South Brazilian dominion and the Chacoan subregion, with a potential distribution mainly restricted to the Neotropics. There is no doubt that the known range of the species lacks information and further records will be found. As more information about the immature stages of Psychodinae is known it will become easier to find specific habitats to find new records and new species (e.g., searching for specific microhabitats).

Biodiversity loss in the Neotropical region is mainly due to the high fragmentation of the habitats, and many species are doomed to disappear (Antonelli 2021). Hence, the importance to fill the distribution gaps in order to increase our understanding of the natural environments and the relationships with the species inhabiting them (Santos & Hoppe 2018). Moreover, these knowledge gaps are usually encumbered by insufficient taxonomical information (e.g., lack of taxonomists, lack of funding, lack of species surveys, and taxonomic impediments) and highlight the importance of both the need for taxonomical works and the usual apathy of governments to support taxonomical initiatives. This is why projects such as “Diversidad de moscas florícolas (Insecta: Diptera) del Ecuador”, together with international collaborations, are crucial to fill the taxonomical gaps in the Neotropical region aiming for a more complete species list and their distribution in the Neotropics.

## Acknowledgments

The present results are part of the Marco contract named “Diversidad de moscas florícolas (Insecta: Diptera) del Ecuador” (MAAEDBI-CM-2021-0167) issued by the Ecuadorian Ministerio del Ambiente y Agua. We are indebted to Isabel Kilian for collecting the specimens used for this study and to Alex Pazmiño-Palomino for helping with the paperwork in Ecuador. We are grateful to Björn Müller for his invaluable help during the DNA extraction, and we are thankful to Björn Rulik for his help uploading the COI sequences to BOLD. SJS extends his gratitude to Greg Curler for enlightening the understanding of some characters in the male genitalia. We are thankful to Danilo Cordeiro and one anonymous reviewer for their comments that improved the final version of our publication.

## References

- Antonelli A. 2021. The rise and fall of Neotropical biodiversity. *Botanical Journal of the Linnean Society* 199: 8–24. <https://doi.org/10.1093/botlinnean/boab061>
- Astrin J.J. & Stüben P.E. 2008. Phylogeny in cryptic weevils: molecules, morphology and new genera of western Palearctic Cryptorhynchinae (Coleoptera: Curculionidae). *Invertebrate Systematics* 22: 503–522.

- Cumming J.M. & Wood D.M. 2017. Adult Morphology and terminology. In: Kirk-Springs A.H. & Sinclair B.J. (eds) *Manual of Afrotropical Diptera. Vol. 1. Introductory Chapters and Keys to Diptera Families*. Suricata 4: 89–133. South African National Biodiversity Institute, Pretoria.
- Fick S.E. & Hijmans R.J. 2017. WorldClim 2: new 1-km spatial resolution climate surfaces for global land areas. *International Journal of Climatology* 37 (12): 4302–4315. <https://doi.org/10.1002/joc.5086>
- HPPC 2015. Plan General Provincial de Desarrollo. Honorable Consejo Provincial de Pichincha – HCPP. Asamblea de Pichincha. Available online from [https://www.epp.gob.ec/ley%20de%20transparencia/rendicioncuentas/2020/1\\_PDOT.pdf](https://www.epp.gob.ec/ley%20de%20transparencia/rendicioncuentas/2020/1_PDOT.pdf) [accessed on 27 Feb. 2024]
- Jaume-Schinkel S. 2022. Description of *Tonnoira conistylus* sp. nov. from Costa Rica and a new record of *Tonnoira distincta* Bravo et al. 2008 from Ecuador. *Studies on Neotropical Fauna and Environment*. <https://doi.org/10.1080/01650521.2022.2081466>
- Jaume-Schinkel S. & Kvitte G.M. 2022. *Platyplastinx ibanezbernali* sp. nov., a new species of moth fly (Diptera: Psychodidae) from Ecuador. *Acta Entomologica Musei Nationalis Pragae* 62 (2): 383–389. <https://doi.org/10.37520/aemnp.2022.020>
- Jaume-Schinkel S., Kvitte G.M., van der Weele R. & Mengual X. 2022. *Alepiea viatrix* sp. nov. (Diptera: Psychodidae), a new species of a Neotropical genus found on the Azores Archipelago (Portugal). *Zootaxa* 5128 (3): 384–396. <https://doi.org/10.11646/zootaxa.5128.3.4>
- Ježek J., Oboňa J., Le Pont F., Maes J.M. & Martinez E. 2020. Redescription of *Armillipora* Quate (Diptera: Psychodidae: Psychodinae) with a new species from Bolivia. *Zootaxa* 4890 (3): 417–427. <https://doi.org/10.11646/zootaxa.4890.3.8>
- Kvitte G.M. 2018. Molecular phylogeny of moth flies (Diptera, Psychodidae, Psychodinae) revisited, with a revised tribal classification. *Systematic Entomology* 43 (3): 596–605. <https://doi.org/10.1111/syen.12288>
- Kvitte G.M. & Wagner R. 2017. Psychodidae (Sand Flies, Moth Flies or Owl Flies) In: Kirk-Spriggs A.H. & Sinclair B.J. (eds) *Manual of Afrotropical Diptera. Vol. 2. Nematoceros Diptera and Lower Brachycera*. Suricata 5. South African National Biodiversity Institute, Pretoria. 607–632.
- Korbie D.J. & Mattick J.S. 2008. Touchdown PCR for increased specificity and sensitivity in PCR amplification. *Nature Protocols* 3: 1452–1456. <https://doi.org/10.1038/nprot.2008.133>
- Lee-Yaw J.A., McCune J.L., Pironon S. & Sheth S.N. 2021. Species distribution models rarely predict the biology of real populations. *Ecography* 2022 (6): e05877. <https://doi.org/10.1111/ecog.05877>
- Phillips S.J., Dudík M. & Schapire R.E. 2023. Maxent software for modeling species niches and distributions (ver. 3.4.1). Available from [http://biodiversityinformatics.amnh.org/open\\_source/maxent/](http://biodiversityinformatics.amnh.org/open_source/maxent/) [accessed on 8 Feb. 2023]
- Quate L.W. 1996. Preliminary taxonomy of Costa Rican Psychodidae (Diptera), exclusive of Phlebotominae. *Revista Biología Tropical* 44 (Supplement 1): 1–81.
- Quate L.W. 1999. Taxonomy of neotropical Psychodidae. (Diptera) 3. Psychodines of Barro Colorado Island and San Blas, Panamá. *Memoirs on Entomology International* 14: 409–441.
- Quate L.W. & Brown B. 2004. Revision of Neotropical Setomimini (Diptera: Psychodidae: Psychodinae). *Natural History Museum of Los Angeles County Contributions in Science* 500: 1–117. <https://doi.org/10.5962/p.210558>
- Santos B.F. & Hoppe J.P.M. 2018. Filling gaps in species distributions through the study of biological collections: 415 new distribution records for Neotropical Cryptinae (Hymenoptera, Ichneumonidae). *Revista Brasileira de Entomologia* 62 (4): 288–291. <https://doi.org/10.1016/j.rbe.2018.09.001>

Stas M., Aerts R., Hendrickx M., Dendoncker N., Dujardin S., Linard C., Nawrot T., Nieuwenhuyse A.V., Aerts J.M., Orshoven J.V. & Somers B. 2020. An evaluation of species distribution models to estimate tree diversity at genus level in a heterogeneous urban-rural landscape. *Landscape and Urban Planning* 198: 130770. <https://doi.org/10.1016/j.landurbplan.2020.103770>

Wagner R. 1981. Two new moth-flies (Diptera, Psychodidae) from South America. *Studies on Neotropical Fauna and Environment* 16: 217–220.

*Manuscript received: 31 May 2023*

*Manuscript accepted: 6 November 2023*

*Published on: 12 March 2024*

*Topic editor: Tony Robillard*

*Section editor: Torbjørn Ekrem*

*Desk editor: Marianne Salaiün*

Printed versions of all papers are also deposited in the libraries of the institutes that are members of the *EJT* consortium: Muséum national d’histoire naturelle, Paris, France; Meise Botanic Garden, Belgium; Royal Museum for Central Africa, Tervuren, Belgium; Royal Belgian Institute of Natural Sciences, Brussels, Belgium; Natural History Museum of Denmark, Copenhagen, Denmark; Naturalis Biodiversity Center, Leiden, the Netherlands; Museo Nacional de Ciencias Naturales-CSIC, Madrid, Spain; Leibniz Institute for the Analysis of Biodiversity Change, Bonn – Hamburg, Germany; National Museum of the Czech Republic, Prague, Czech Republic.